7B.6

AIRCRAFT OBSERVATIONS OF THE ATMOSPHERIC BOUNDARY LAYER OVER THE RONNE POLYNYA, SOUTHERN WEDDELL SEA, ANTARCTICA

E. K. Fiedler*, I. A. Renfrew
University of East Anglia, Norwich, UK
T. A. Lachlan-Cope, J. C. King
British Antarctic Survey, Cambridge, UK

1 INTRODUCTION

The Ronne Polynya is a wind-driven coastal polynya, which is a region of thin ice or open water in pack ice, caused by the continual offshore advection of the ice by strong continental winds as quickly as it can form, see fig. 1. These polynyas are sites of significant air-sea-ice interactions, thereby having an important impact on both the regional meteorology and oceanography of the high latitudes.

Due to the exposed ocean surface, ocean-atmosphere temperature and humidity differences are large, resulting in large sensible and latent heat fluxes. This leads to a warming and moistening of the atmospheric boundary layer above and downwind of the polynya and, through vigorous convective mixing, the formation of a CIBL (convective internal boundary layer). This warming and moistening causes a decrease in the ocean-atmosphere temperature and humidity gradients, which results in a decrease in the surface heat fluxes with fetch from the shore, or ice shelf front (e.g. Renfrew and King, 2000).

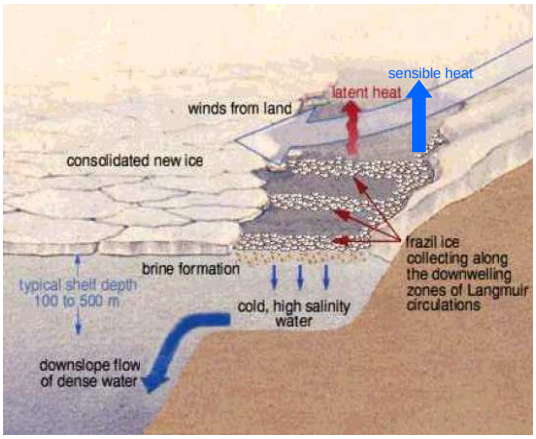

Figure 1: *Coastal polynya formation mechanism (after Open University, 1998). When winds become light or onshore the polynya freezes over.*

As well as this turbulent heat transfer, polynyas can also influence the balance of radiative heat transfer through the generation of ice fog (Smith et al., 1990) and convective clouds or plumes (Pinto and Curry, 1995). Polynyas therefore have the potential to modify and induce

* *Corresponding author address:* Emma Fiedler, University of East Anglia, School of Environmental Sciences, Norwich, UK, NR4 7TJ; email: e.fiedler@uea.ac.uk

mesoscale atmospheric motion, impacting on regional climate (Pinto et al., 1995).

The large ocean-atmosphere heat fluxes and the continual removal of the ice by the wind result in high rates of ice production, earning this type of polynya the nickname "ice factory". This continuous ice formation results in extensive brine rejection, increasing the salinity and therefore the density of the water column. This dense water accumulates on the continental shelf, and in the case of the Ronne Polynya, forms a water mass known as High Salinity Shelf Water (HSSW) which, through a number of pathways, leads on to the formation of Antarctic Bottom Water (AABW), the most widespread water mass in the global ocean. This ice formation mechanism within polynyas is therefore important for the ventilation of deep and bottom water in both the Southern and Arctic Oceans.

Quantification of the surface heat budget, together with the surface salinity budget, will aid understanding of the key processes governing deep water formation within polynyas. For this purpose, the ocean-atmosphere sensible heat fluxes at the Ronne Polynya, Antarctica, were investigated using a combination of fieldwork observations and modelling.

2 OBSERVATIONS

The Ronne Polynya is located adjacent to the Ronne Ice Shelf in the southern Weddell Sea, Antarctica, see fig. 2. It is a recurring polynya, meaning it opens episodically in the same location, appearing when the wind is directed off the ice shelf. Its surface area is approximately $20 \times 10^3\ km^2$, with an offshore fetch of the order of 100 km, but with large inter- and intra-seasonal variability (Renfrew et al., 2002).

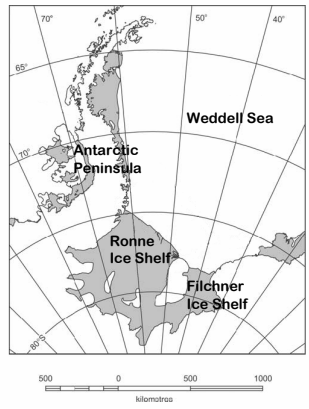

Figure 2: *Study location.*

Using a British Antarctic Survey (BAS) instrumented twin otter aircraft, high frequency wind and temperature data from three flights over the Ronne Polynya were collected between 25 and 28 February 2007, during a cold air outbreak off the Ronne Ice Shelf caused by the presence of a low pressure system situated in the Weddell Sea. In total, four low altitude legs were conducted in the along-wind direction, perpendicular to the ice shelf. Details of these flights are given in table 1, where a leg 1 (L1) represents a flight out from the ice shelf and a leg 2 (L2) towards.

It is assumed conditions were steady and homogeneous and therefore the surface layer of the CIBL was a constant flux layer. At an altitude of $14 - 33\ m$ the plane was assumed to be flying within this layer and so it was not necessary to extrapolate flux values to the surface.

The Ronne Polynya flights were part of a larger BAS fieldwork campaign, measuring surface fluxes over open water, sea ice and ice shelves around the

Flight	Date and time	Mean altitude (m)	Fetch (km)	T_s - T_{air} (^oC) range	10 m wind speed (ms^{-1}) range	Mean wind direction range (offshore ≈ 180-225)
F49L2	25/02/07 16:52 - 17:17	32	84.9	2.1 - 9.0	4.8 - 6.6	195.9 - 208.1
F54L1	27/02/07 15:18 - 15:43	14	120.9	3.1 - 12.8	13.3 - 16.3	204.0 - 213.5
F54L2	27/02/07 15:44 - 16:27	33	127.5	2.9 - 12.5	8.0 - 11.5	196.0 - 208.8
F57L1	28/02/07 16:32 - 16:59	15	85.2	4.4 - 14.0	11.5 - 12.3	212.5 - 220.6

Table 1: Flight Information

Antarctic Peninsula. Figure 3 shows all the flight tracks for the season, including the three flights over the Ronne Polynya.

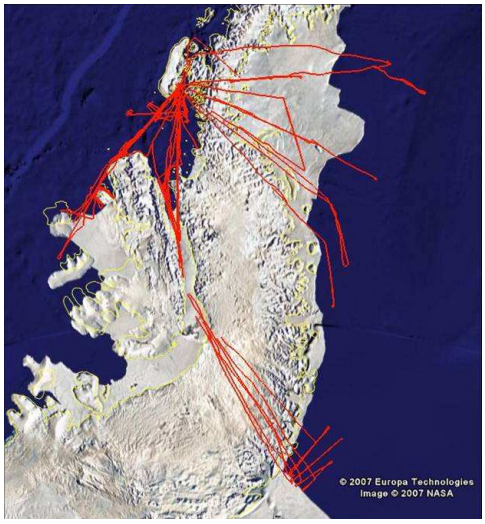

Figure 3: *Flight tracks*

A Best Aircraft Turbulence, or BAT, probe (Garman et al., 2006) was used to collect measurements of temperature and wind speed at a frequency of 50 Hz for direct measurement of surface eddy covariance heat and momentum fluxes.

Low frequency measurements were made using instruments including an infra-red radiometer for measuring surface temperature, a cooled mirror hygrometer and humicap sensor for measuring humidity and pyranometers and pyrgeometers for measuring upwelling and downwelling radiation. All data were recorded using an onboard computer system. Figure 4 shows the plane, where the BAT probe can be seen mounted on a boom extending in front of the nose of the plane.

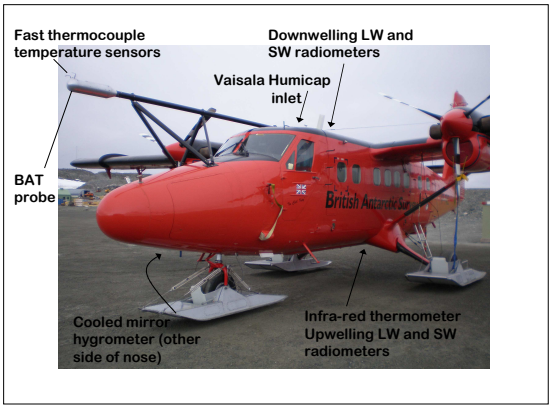

Figure 4: *The research plane, showing the onboard location of the instruments.*

Quality control procedures to investigate the reliability of the data included examination of the power spectra for the individual flux components,

the cumulative summation of the covariances, as well as the cospectra and ogives (e.g. Friehe et al., 1991; French et al., 2007). This also indicated that the selected averaging period, or run, of 140 seconds was appropriate for capturing the turbulent wavelengths. Seven flux runs out of a total of 49 were discarded on the basis of the above analysis. One run was also rejected due to an instrument malfunction.

3 RESULTS

3.1 Eddy covariance sensible heat fluxes

The surface sensible heat fluxes with fetch from the ice shelf were calculated using the eddy covariance method (e.g. Busch, 1973), where the sensible heat flux is given by

$$Q_S = \rho c_p \overline{w'T'} \tag{1}$$

where ρ is the air density, c_p is the specific heat capacity of air, and w' and T' are vertical wind speed and temperature perturbations respectively. The bar denotes the mean value of the covariance over the averaging period, chosen here to be 140 seconds.

Figure 5 shows the eddy covariance sensible heat fluxes over the Ronne Polynya for F54L1 with fetch from the ice shelf edge at 0 km. The surface temperature, air potential temperature and albedo are also shown for this flight leg and are all averaged over the same 140 second non-overlapping intervals.

A decrease in the sensible heat fluxes with fetch is observed due to a reduction in the air-surface temperature difference. This is due in part to the warming of the CIBL by sensible heat flux convergence, including entrainment of warm air from above. However, for these case studies, the polynya was observed to be mostly covered with thin ice which increased in thickness with increasing fetch from the ice shelf edge, and no large areas of open water were present. This is illustrated on the plot of surface albedo, see fig. 5, where the higher the albedo, the thicker the ice cover. The decrease in surface temperature with fetch due to the thickening ice cover was greater than the observed increase in air temperature due to warming, as can also be seen on fig. 5. This means that for this case it is the changing surface temperature of the inhomogeneous surface, and not the air temperature, which has the greatest effect on the surface-air temperature difference and consequently on the spatial variability of the sensible heat flux. This was also the situation for the other flux legs.

3.2 Surface Regimes

As described by Morales Maqueda et al. (2004), two regions can be distinguished in a wind-driven polynya, corresponding to an inner region of open water and frazil ice and an outer region of new and young ice floes formed by frazil ice accretion, which is surrounded by first-year ice. These regions are referred to by Liu et al. (1997) as the "active polynya" and "young ice" regions respectively. In this study, both regions are considered to be part of the polynya.

The thickening surface ice cover observed over the Ronne Polynya can be split into two distinct areas, or regimes, which correspond to these two

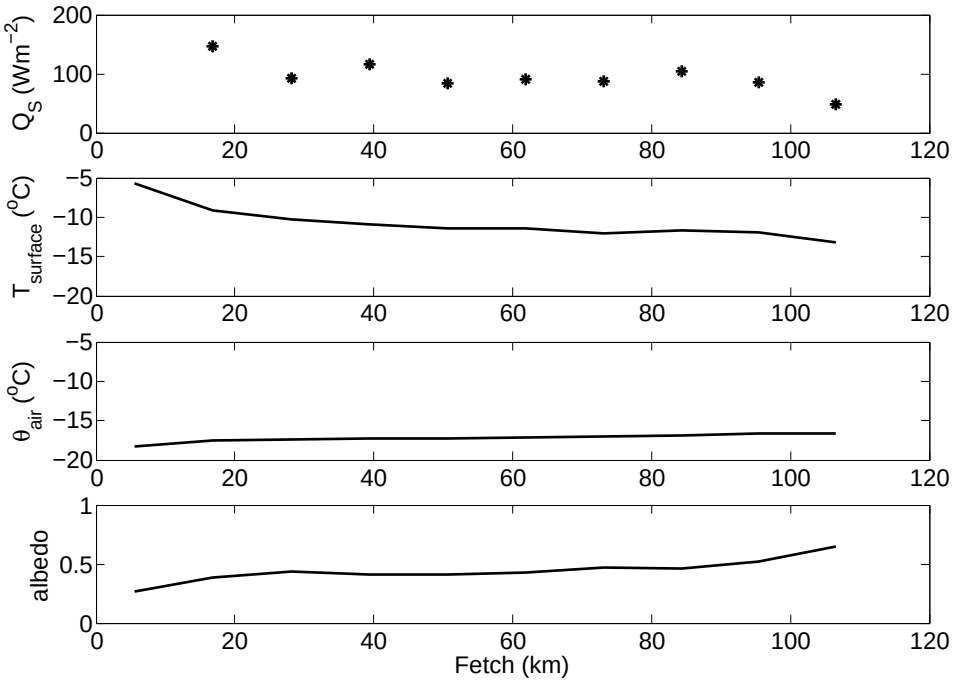

Figure 5: *For F54L1. Top to bottom: eddy covariance sensible heat flux, surface temperature, air potential temperature and surface SW albedo, all with fetch from polynya edge.*

regions. They can be clearly identified on figure 6, which shows the surface shortwave albedo and surface temperature frequency distribution for F54L1 and F54L2.

Figure 7 shows photographs of typical surface conditions observed within the regimes for these cases. The first regime, figure 7(a), or the active polynya, corresponds to open water and frazil ice. Langmuir circulations are observed in the surface distribution pattern of the frazil ice, as well as some slightly thicker new ice. This regime covers the first 30 km for F54. The second regime, figure 7(b), or the young ice region, corresponds to more consolidated ice with 'holes'. Heat fluxes over the second regime are still around 100 Wm^{-2} and so this area is still considered to be part of the polynya.

3.3 Transfer Coefficients

If high frequency data are not available, surface fluxes can be parameterised using the bulk aerodynamic formulae. The bulk sensible heat flux is given by (e.g. Hartmann, 1994)

$$Q_S = \rho c_p C_{Hr} U_r (T_{sfc} - \Theta_r) \qquad (2)$$

Subscripts sfc and r respectively denote the surface and the reference height. Fluxes are positive upwards and c_p and ρ are as given previously. T is the temperature, Θ the potential temperature, U the wind speed and z the measurement height.

C_H is the empirically-determined coefficient for

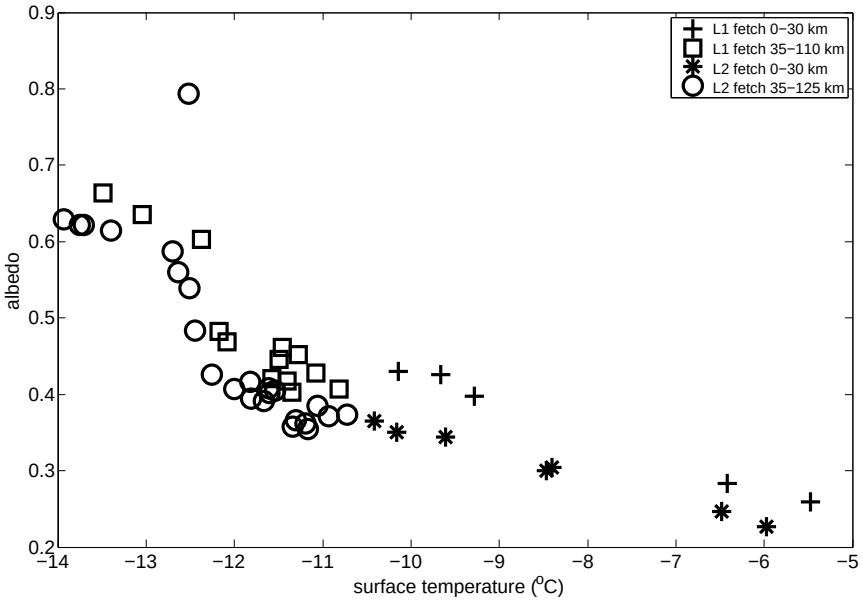

Figure 6: *5 km averaged SW albedo and surface temperature for F54L1 and F54L2, split into regimes where first regime is first 30 km.*

sensible heat transfer. Calculation of sensible heat fluxes by this method therefore requires accurate determination of this transfer coefficient appropriate to the surface. Using equation 1 together with equation 2 yields equation 3, into which the Ronne Polynya observations were substituted to determine values for this coefficient at the measurement, or reference height. Using a similar method, the drag coefficients were also obtained (equation 4).

$$C_{Hr} = \frac{\overline{w'T'}}{U_r(T_s - \Theta_r)} \tag{3}$$

$$C_{Dr} = \frac{\left(\overline{u'w'} + \overline{v'w'}\right)^{1/2}}{U_r^2} \tag{4}$$

In order to compare measurements made under different stratification conditions and at different measurement heights, values of the bulk coefficients were then converted to equivalent neutral stability values at a reference height of 10 m.

Following Andreas and Cash (1999):

Neutral stability drag coefficient at 10 m height

$$C_{DN10} = \frac{C_{Dr}}{\left\{1 - \kappa^{-1} C_{Dr}^{1/2} \left[ln(r/10) - \Psi_m(r/L)\right]\right\}^2} \tag{5}$$

$$C_{HN10} = \frac{C_{Hr}}{\left(C_{Dr}/C_{DN10}\right)^{1/2} - \kappa^{-1} C_{Hr} C_{DN10}^{-1/2} \left[ln(r/10) - \Psi_h(r/L)\right]} \tag{6}$$

where the Obukhov length, L, is given by

$$L = \frac{\overline{T}_v u_*^3}{-\kappa g \overline{w' t_v'}}$$

u_* is the friction velocity, given by

$$u_* = \left(\overline{u'w'}^2 + \overline{v'w'}^2\right)^{1/4}$$

κ is von Karman's constant (0.4) and g is acceleration due to gravity (9.81 ms^{-2}).

(a) F54 First regime

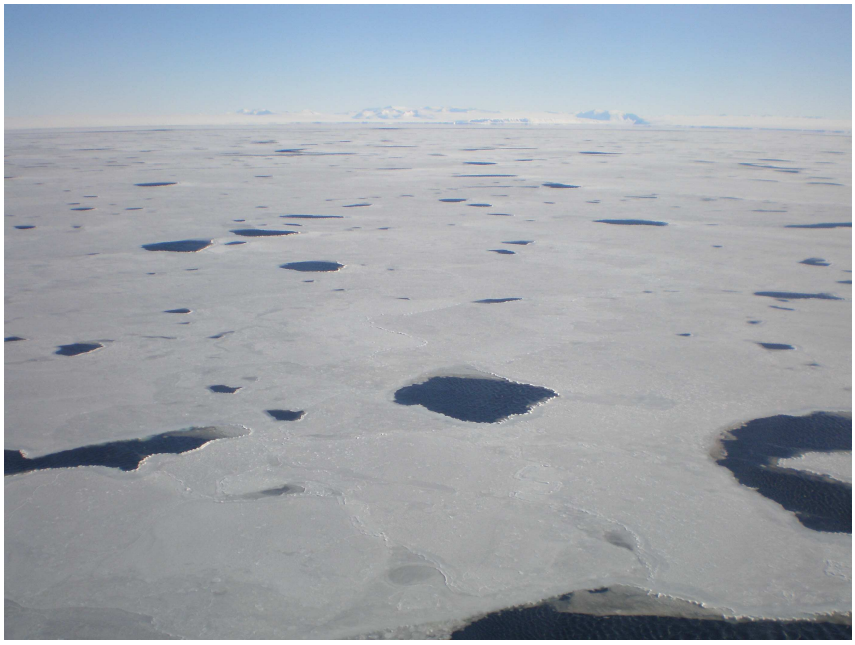

(b) F54 Second regime

Figure 7: *Photographs of Ronne Polynya surface from plane at altitude of approximately 15 m.*

$\overline{T}_v = \overline{T}(1 + 0.61\overline{q})$

where $\overline{T}$ and $\overline{q}$ are representative values of temperature and specific humidity in the CIBL.

$\overline{w't'_v} = \overline{w't'}(1 + 0.61\overline{q}) + 0.61\overline{T}\ \overline{w'q'}$

where

$\overline{w'q'} = \frac{c_p}{L_v}\frac{\overline{w't'}}{Bo}$

and Bo is the Bowen Ratio, where for simplicity $C_H = C_E$ is assumed, giving

$Bo = \frac{c_p}{L_v}\frac{(T_s - \Theta_r)}{(q_s - q_r)}$

Ψ_m and Ψ_h are non-dimensional stability functions, set as the commonly used Businger-Dyer flux profile relations for variation with stability in the profiles of wind and temperature (e.g. Businger et al., 1971; Dyer, 1974).

The ratio r/L, or ζ, is the stability parameter, where $\zeta > 0$ indicates stable stratification, $\zeta < 0$ indicates unstable stratification and $\zeta = 0$ under neutral conditions.

For the neutral case,

$$\Psi_m(\zeta) = \Psi_h(\zeta) = 0$$

For stable stratification (Dyer, 1974)

$$\Psi_m(\zeta) = \Psi_h(\zeta) = -\alpha\frac{r}{L}$$

where $\alpha = 5$.

For unstable stratification (Paulson, 1970)

$$\Psi_m(\zeta) = 2ln[(1+x)/2] + ln[(1+x^2)/2] - 2tan^{-1}x + \pi/2$$

$$\Psi_h(\zeta) = 2ln[(1 + x^2)/2]$$

where $x = (1 - 16\zeta)^{\frac{1}{4}}$.

Values of the transfer coefficients obtained from the two lower level legs only (i.e. F54L1 and F57L1) were used due to the increased scatter in the flux data collected at the higher altitudes. Figure 8 shows the 10 m neutral stability heat transfer and drag coefficients calculated for each 140 s period, shown with fetch from the ice shelf edge at 0 km. Despite the data being collected more than 24 hours apart, the mean values of these coefficients for both of the legs are very similar, at $C_{DN10} = 1.10 \times 10^{-3}$ for both legs and $C_{HN10} = 0.72 \times 10^{-3}$ for F54L1 and $C_{HN10} = 0.68 \times 10^{-3}$ for F57L1.

The observed values of the coefficients are within the range of previous comparable observations, but towards the lower end. For example, Andreas et al. (2005) give values of C_{DN10} of 1.0 - 2.0$\times 10^{-3}$, dependent on the surface ice concentration, and Andreas and Murphy (1986) give values for C_{HN10} of 1.0$\times 10^{-3}$. However, there are no similar aircraft-based observational data sets which have been collected over an ice covered polynya in the Antarctic, illustrating the uniqueness of these observations.

Neither the drag nor the heat transfer coefficients were found to be a function of fetch, as can be observed on figure 8, i.e. there is no correlation between fetch and C_{DN10} or C_{HN10} at either the 0.01 or 0.05 significance levels. Similarly, a t-test shows there is no significant difference between the means of the transfer coefficients for the different regimes. It can therefore be concluded that, for these case studies, the two ice regimes transfer heat and momentum similarly, which suggests that under similar polynya conditions, the two ice regimes can be treated in the same way when modelling the surface heat fluxes.

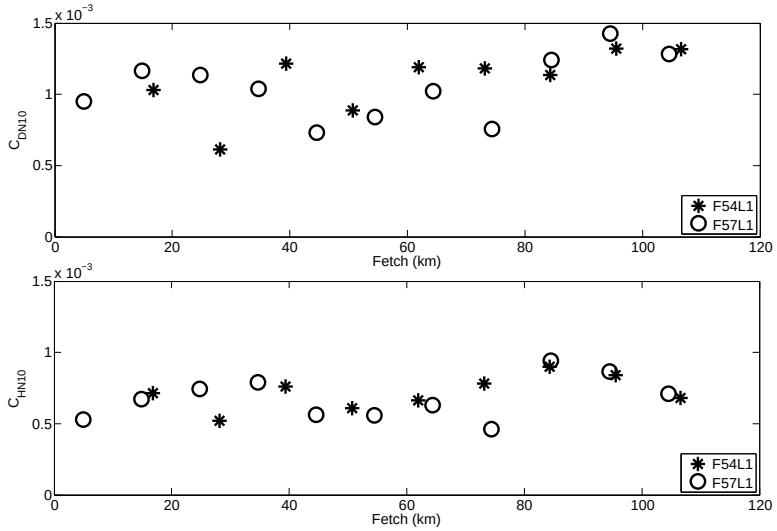

Figure 8: *10 m neutral stability drag and heat transfer coefficients for F54L1 and F57L1.*

As indicators of the surface ice type, relationships between these coefficients and the surface shortwave albedo and the surface temperature were also investigated (figure 9). No significant correlations were found, either when considering all the data together, or when splitting it into the two regimes.

There may be a linear relationship for the transfer coefficients with surface temperatures above about -10 ^oC, but the range of data is limited, since most of the Ronne Polynya measurements lie between surface temperatures of -10 and -12 ^oC and albedos of 0.4 to 0.5. Therefore, to more fully examine any (possibly non-linear) relationship between surface ice type or concentration and these coefficients, a wider spread of data would be required.

Based on measurements made in the Arctic, Andreas et al. (2005) suggest that at high ice concentrations a heterogeneous surface of ice and open water (whether leads, gaps between floes or melt ponds) can behave aerodynamically as if it were fairly homogeneous, resulting in little variation in C_{DN10}. Therefore values of C_{DN10} might be expected to depend on ice concentration rather than ice thickness or type.

Therefore, it can be inferred for the Ronne Polynya case studies that although the surface temperature drops as the ice becomes thicker, the actual ice concentration remains high enough that the drag coefficient is not a function of fetch or surface ice regime, and therefore neither is the neutral stability heat transfer coefficient.

4 MODELLING OF SENSIBLE HEAT FLUXES

The observational data collected over the Ronne Polynya were used to provide initial conditions for

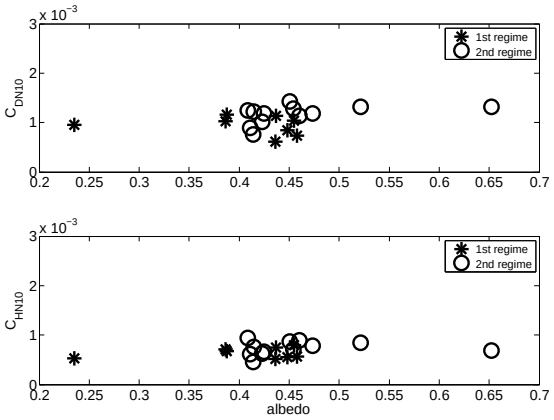

(a) 10 m neutral stability drag coefficient (top) and heat transfer coefficient (bottom) with surface shortwave albedo

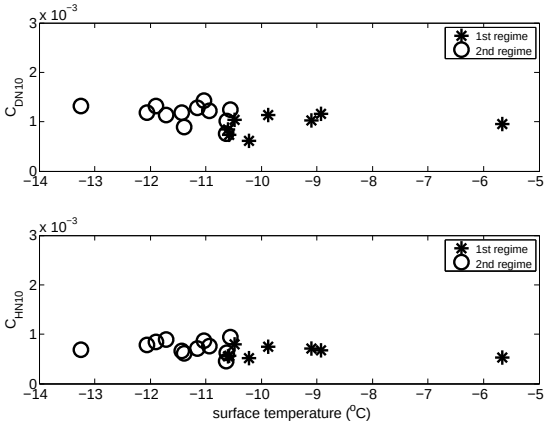

(b) 10 m neutral stability drag coefficient (top) and heat transfer coefficient (bottom) with surface temperature

Figure 9: *F54L1 and F57L1 transfer coefficients with surface shortwave albedo (a), and surface temperature (b). Data split into the two ice regimes.*

a one-dimensional slab model of the CIBL. The model allows the surface sensible heat flux, boundary layer height and mixed-layer potential temperature to vary with fetch. Full model details are given in Renfrew and King (2000).

The model was designed for the simple case of an open water polynya with a constant surface temperature. However, as discussed above, at the time of the case studies the Ronne Polynya was observed to be mostly covered with thin ice which increased in thickness with fetch, and therefore a consequent reduction in surface temperature with fetch was found. A two-regime surface temperature was therefore introduced to the model, using the mean value for each regime.

Other appropriate changes were made to the model, including the removal of the Charnock parameter, as there was found to be no dependence of the surface roughness length on the wind speed for these case studies.

Additionally, the mean value for C_{HN10} calculated above was used. The model default C_{DN10} (1.0×10^{-3} (Smith, 1988)) was similar to that calculated from the Ronne Polynya observations (1.1×10^{-3}).

Initial conditions at the ice shelf edge (0 km) of wind speed, air potential temperature (θ), surface temperature and pressure as well as atmospheric stability and the entrainment parameter (ratio of the entrainment heat flux at the top of the boundary layer to the surface turbulent heat flux) were specified using the observational data obtained during F54. The values used for the model runs are given in table 2.

Figure 10 shows the modelled sensible heat fluxes with fetch, with the observed eddy covariance sensible heat fluxes for F54L1 and F54L2.

Using a single regime for the surface temperature captures the first regime sensible heat fluxes well but overestimates the heat fluxes for the second regime by around 50 Wm^{-2}. Therefore, rather than inputting the surface temperature for each model point, this two-regime method preserves the simplicity of the model but is more accurate than using a single, constant surface temperature, and gives comparable results to inputting the observed surface temperature at each point. This is more useful for modelling applications where high resolution surface data may not be available.

Use of a two-regime surface temperature has less of an effect on the modelled heat fluxes for F49 and F57 as there is a smaller temperature difference between the two regimes. Therefore, the importance of a two-regime temperature input is dependent upon the magnitude of the mean surface temperature difference between regimes.

The use of a single value of both the heat transfer and drag coefficients for modelling both regimes has produced accurate results, therefore reinforcing the result found above that there is no significant difference in the transfer coefficients between regimes.

For comparison purposes, the model was also run assuming the polynya consisted of open water at the freezing point, at a temperature of -1.9 ^oC. The Charnock parameter and the original model transfer coefficients of $C_{DN10} = 1.0 \times 10^{-3}$ (Smith, 1988) and $C_{HN10} = 1.14 \times 10^{-3}$ (DeCosmo et al., 1996) were also reintroduced. Results are also shown on figure 10.

The model was also run assuming the polynya was open water as above but using the Ronne

wind speed	θ_{air}	T_{sfc} regime 1	T_{sfc} regime 2	pressure	ambient stability	entrainment parameter
17 ms^{-1}	-18.8 ^oC	-7.8 ^oC	-11.4 ^oC	994 mb	6 Km^{-1}	0.5

Table 2: Model input data from aircraft observations

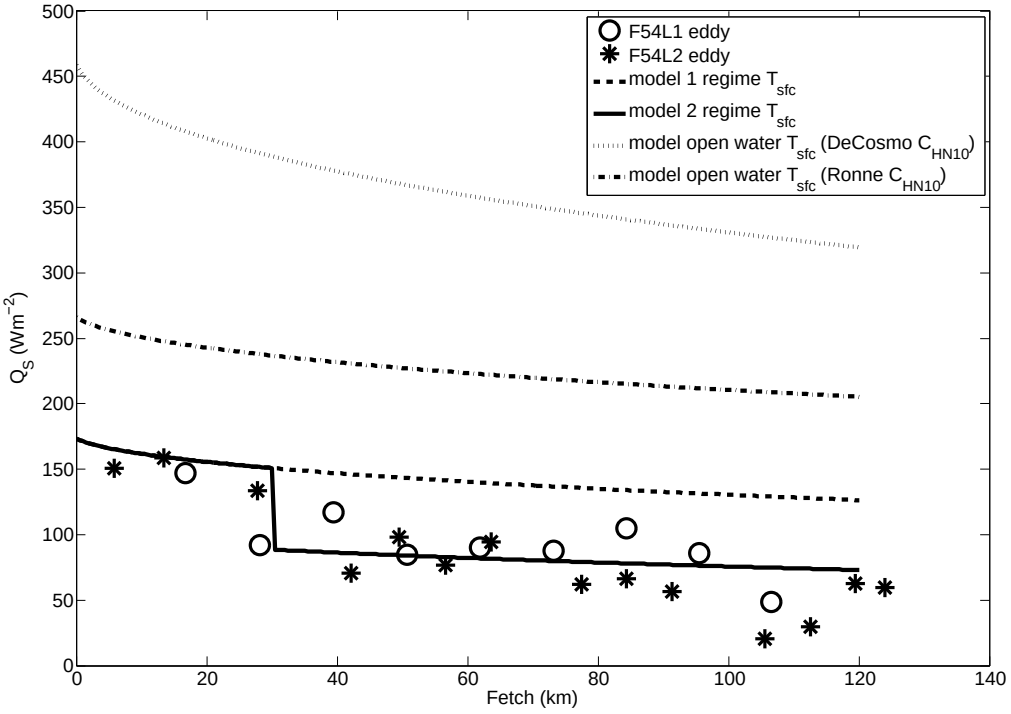

Figure 10: *F54 observed eddy sensible heat flux for L1 and L2, and modelled sensible heat flux shown with variations in surface temperature and heat transfer coefficent.*

Polynya transfer coefficients. It can be seen that the modelled sensible heat flux is not only sensitive to the precribed surface temperature but also to the value of the transfer coefficients. Errors in either parameter could therefore result in a large over- or underestimate of the modelled surface sensible heat fluxes.

Therefore, to accurately model the sensible heat flux, for these case studies the polynya should be treated as ice-covered and the appropriate surface temperature (two-regime, to account for large variation in fetch) and transfer coefficients (which are applicable to both regimes) should be used. It can therefore be inferred that under similar conditions where high polynya ice formation rates are expected (large air-sea temperature differences, rapid offshore advection of new ice) heat fluxes over any wind-driven coastal polynya could be modelled in the same way.

Figure 11 is an image of satellite-derived ice concentration for the day of F54 (27 February 2007), using AMSR-E (Advanced Microwave Scanning

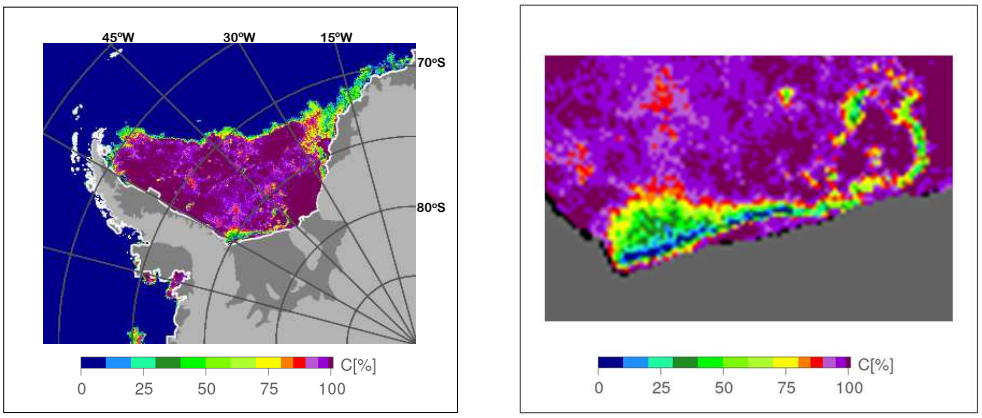

Figure 11: *Left: AMSR-E sea-ice concentration 27-Feb-2007, grid 6.25 km (Spreen et al., 2008). Low ice concentrations can be seen at the Ronne Polynya (around 75° S, 60° W), see zoomed-in image (right).*

Radiometer for EOS) data. The Ronne Polynya can be identified as the area of low ice concentration situated off the Ronne Ice Shelf and the two ice regimes can clearly be seen. The AMSR-E ice concentration for the first regime is given as 0-10%. However, the in-situ data has shown that this ice concentration was greater than 0% (open water) reducing the heat transfer coefficient and surface temperature accordingly. Therefore, if in-situ data were not available, the assumption, using this satellite data, that this regime could be modelled as open water, would lead to a significant overestimate in the modelled sensible heat fluxes.

5 CONCLUSIONS

5.1 Observations

Unique data from low-level aircraft-based observations of turbulence over the Ronne Polynya, Antarctica, have been presented. Limited data exists over polynyas, especially in the Antarctic. The surface sensible heat fluxes were found to decrease with fetch from the edge of the ice shelf due to a reduction in the surface-air temperature difference. This was primarily a result of thickening ice cover with fetch and a consequent decrease in the surface temperature, although there was some contribution from the increase in air temperature due to warming of the CIBL.

The polynya was observed to be mostly covered with thin ice at the time of the case studies. This ice cover can be split into two distinct regimes, corresponding to new ice and more consolidated new ice. Both of these regimes are considered to be part of the polynya due to the large heat fluxes observed and the similarity of the values of both the heat transfer and drag coefficients for the two regimes. New values for the 10 m neutral stability heat transfer and drag coefficients were calculated, and were found to not be a function of polynya fetch. The mean values of these coefficients are $C_{DN10} = 1.1 \times 10^{-3}$ and $C_{HN10} = 0.7 \times 10^{-3}$. No significant difference in the values of the coefficients for the two ice regimes was found and they

can therefore be assumed to transfer heat and momentum similarly.

These results are applicable to thin ice-covered wind-driven polynyas in general, in both the Antarctic and the Arctic as well.

5.2 Modelling

At the time of these case studies, the Ronne Polynya was observed to be mostly covered with thin ice, rather than being open water. Therefore, modelling of the sensible heat fluxes over the polynya under these conditions requires values of the surface temperature and transfer coefficients appropriate to an ice surface, and no Charnock parameter is required. If the variation in surface temperature with fetch is large, a two-regime surface temperature is appropriate. The transfer coefficients are however applicable to both regimes.

It can be inferred that under similar conditions, where ice formation rates are expected to be high (large air-sea temperature differences, rapid offshore advection of new ice), heat fluxes over other wind-driven coastal polynyas can be modelled in the same way. If ice formation rates are lower, meaning there are large areas of open water in the first regime area, a surface temperature and transfer coefficients appropriate for open water would need to be used and the Charnock parameter reintroduced.

Therefore, for modelling of convective heat transfer over polynyas, the distinction between open water and thin ice within the first regime is an important one. This also has implications for problems such as whether, for satellite ice concentration algorithms, to consider the thin ice of polynyas in the same way as the thicker ice of the second regime or as open water. This study would suggest that the thin ice should be considered in the same way as the thicker ice of the second regime, due to the reduction in the sensible heat flux compared to open water and the similarity of the transfer coefficients to the second regime.

It is therefore important to note for modelling of the surface sensible heat flux whether the polynya regime is open water, thin ice or more consolidated ice to accurately assess the effect of polynyas on the ocean-atmosphere heat fluxes and on the regional oceanography and meteorology of the high latitudes.

References

Andreas, E. L. and Cash, B. A. 1999. Convective heat transfer over wintertime leads and polynyas. *J. Geophys. Res*, 104(C11):25721–25734.

Andreas, E. L. and Murphy, B. 1986. Bulk transfer co-efficients for heat and momentum over leads and polynyas. *J. Phys. Oceanogr.*, 108:1875–1883.

Andreas, E. L., Persson, P. O. G., Jordan, R. E., Horst, T. W., Guest, P. S., Grachev, A. A., and Fairall, C. W. 2005. Parameterizing the turbulent surface fluxes over summer sea ice. In *8th Conference on Polar Meteorology and Oceanography*, page J1.15.

Busch, N. 1973. On the mechanics of atmospheric turbulence. In Haugen, D., editor, *Workshop on Micrometeorology*, pages 1–65, Boston, Mass. American Meteorological Society.

Businger, J. A., Wyngaard, J., Izumi, Y., and Bradley, E. 1971. Flux-profile relationships in the atmospheric surface layer. *J. Atmos. Sci.*, 28:181–189.

DeCosmo, J., Katsaros, K. B., Smith, S. D., Anderson, R. J., Oost, W. A., Bumke, K., and Chadwick, H.

1996. Air-sea exchange of water vapor and sensible heat: The humidity exchange over the sea (hexos) results. *J. Geophys. Res*, 101:12001–12016.

Dyer, A. 1974. A review of flux-profile relationships. *Bound.-Lay. Meteorol.*, 7:363–372.

French, J. R., Drennan, W., Zhang, J., and Black, P. 2007. Turbulent fluxes in the hurricane boundary layer. part i: Momentum flux. *J. Atmos. Sci.*, 64:1089–1102.

Friehe, C., Shaw, W., Rogers, D., Davidson, K., Large, W., Stage, S. A., Crescenti, G., Khalsa, J., Greenhut, G., and Li, F. 1991. Air-sea fluxes and surface layer turbulence around a sea surface temperature front. *J. Geophys. Res.*, 96(C5):8593–8609.

Garman, K., Hill, K., Wyss, P., Carlsen, M., Zimmerman, J., Stirm, B., Carney, T., Santini, R., and Shepson, P. 2006. An airborne and wind tunnel evaluation of a wind turbulence measurement system for aircraft-based flux measurements. *J. Atmos. Ocean. Tech.*, 23:1696–1708.

Hartmann, D. L. 1994. The energy balance of the surface. In *Global Physical Climatology*, volume 56 of *International Geophysical Series*, page 408. Academic Press, London.

Liu, A., Martin, S., and Kwok, R. 1997. Tracking of ice edges and ice floes by wavelet analysis of SAR images. *J. Atmos. Ocean. Tech.*, 14(5):1187–1198.

Morales Maqueda, M. A., Wilmott, A. J., and Biggs, N. R. T. 2004. Polynya dynamics: A review of observations and modeling. *Rev. Geophys.*, 42(1):Art. No. RG1004.

Open University, . 1998. *Ocean Circulation*. Butterworth-Heinemann, Oxford.

Paulson, C. 1970. The mathematical representation of wind speed and temperature profiles in the unstable atmospheric surface layer. *J. Appl. Meteorol.*, 9:857–861.

Pinto, J. O. and Curry, J. A. 1995. Atmospheric convective plumes emanating from leads 2. Microphysical and radiative processes. *J. Geophys. Res.*, 100(C3):4633–4642.

Pinto, J. O., Curry, J. A., and McInnes, K. L. 1995. Atmospheric convective plumes emanating from leads. 1. Thermodynamic structure. *J. Geophys. Res*, 100(C3):4621–4631.

Renfrew, I. A. and King, J. C. 2000. A simple model of the convective internal boundary layer and its application to surface heat flux estimates within polynyas. *Bound.-Lay. Meteorol.*, 94:335–356.

Renfrew, I. A., King, J. C., and Markus, T. 2002. Coastal polynyas in the southern Weddell Sea: Variability of the surface energy budget. *J. Geophys. Res.*, 107(C6):3063, doi:10.1029/2000JC000720.

Smith, S. D. 1988. Coefficients for sea surface wind stress, heat flux, and wind profiles as a function of wind speed and temperature. *J. Geophys. Res*, 93:15467–15472.

Smith, S. D., Muench, R. D., and Pease, C. H. 1990. Polynyas and leads: An overview of physical processes and environment. *J. Geophys. Res.*, 95:9461–9479.

Spreen, G., Kaleschke, L., and Heygster, G. 2008. Sea ice remote sensing using AMSR-E 89 GHz channels. *J. Geophys. Res*, 113:C02S03 doi:10.1029/2005JC003384.